Proc. NIPR Symp. Upper Atmos. Phys., 4, 20–41, 1991

AN EXPERIMENTAL STUDY OF THE ROLE OF HISS IN THE GENERATION OF CHORUS IN THE OUTER MAGNETOSPHERE, AS BASED ON SPECTRAL ANALYSES AND DIRECTION FINDING MEASUREMENTS ONBOARD GEOS 1

Katsumi HATTORI[1], Masashi HAYAKAWA[1], Dominique LAGOUTTE[2], Michel PARROT[2] and François LEFEUVRE[2]

[1]*Solar-Terrestrial Environment Laboratory, Nagoya University, 13, Honohara 3-chome, Toyokawa 442*
[2]*Laboratoire de Physique et Chimie de l'Environnement, CNRS, Orleans Cedex 2, France*

Abstract: The satellite and ground VLF data have indicated that chorus is often accompanied by a background hiss, and the purpose of this paper is to investigate the association between hiss and chorus and to present detailed experimental findings on the cause and effect relationship between hiss and chorus. The present study is based on detailed spectral analyses and direction finding measurements for VLF emission events with the simultaneous occurrence of hiss and chorus observed by GEOS-1 satellite in the outer magnetosphere. Two different events are analyzed: one is the equatorial (geomag. lat. $=6.8°$–$8.5°$) event, and the other the off-equatorial ($24.2°$–$23.6°$) event.

The following important experimental findings have emerged from the present study: (1) Each chorus element originates from the hiss band and is asymptotic to the hiss band. (2) The intensity and occurrence of chorus emissions are closely correlated with the intensity of the underlying hiss band, such that when the intensity of the hiss band exceeds a threshold value of some $m\gamma/\sqrt{Hz}$, the excitation of chorus emission is enhanced. (3) Some parts of hiss band exhibit some structures or wavelets (*i.e.* monochromatic wave components with duration of more than 100 ms), although hiss has been considered to be incoherent and turbulent. Furthermore, on some occasions, we can notice an existence of wavelets at the foot of chorus elements. (4) The direction finding results have newly indicated similar values for the azimuthal direction ϕ for both phenomena, suggesting that both hiss and chorus come from the same source region. These experimental facts suggest that a wavelet existing in the hiss band may generate a chorus emission through coherent wave-particle interaction in the outer magnetosphere as in the case of active VLF wave injection experiments.

1. Introduction

Naturally occurring magnetospheric VLF/ELF emissions are known to be basically classified into two different forms; (1) unstructured hiss (HELLIWELL, 1965; DOWDEN, 1971; HAYAKAWA *et al.*, 1984, 1986a, b, c) and (2) structured and discrete emissions collectively called "chorus" (HELLIWELL, 1965; BURTON and HOLZER, 1974; TSURUTANI and SMITH, 1974; BURTIS and HELLIWELL, 1976; HAYAKAWA *et al.*, 1984, 1986c, 1990).

However, the fundamental problems such as whether these two types of emissions are essentially different or not and the link between hiss and chorus, remain quite unclarified. The phenomenon suitable for studying these unsolved problems is so-called hiss-triggered chorus emissions. The ground and satellite VLF/ELF measurements have indicated that chorus is often accompanied by a background of hiss (BURTIS and HELLIWELL, 1976; CORNILLEAU-WEHRLIN *et al.*, 1978; KOONS, 1981), although chorus is, on many occasions, spontaneously generated (*e.g.*, HELLIWELL, 1965). Another possible stimulus to trigger a chorus is pointed out by LUETTE *et al.* (1977, 1979) to be power line harmonic radiation (PLHR), and they have concluded that man-made VLF noise such as PLHR plays an important role in triggering chorus. But, this hypothesis has been questioned by TSURUTANI *et al.* (1979) and negatively answered by the experimental study of KOONS (1981). Hence, two opposite possibilities have been suggested; one is hiss considered to be incoherent and turbulent, and the other is monochromatic and coherent PLHR. By using the events of hiss-triggered chorus observed onboard the SCATHA satellite, KOONS (1981) has arrived at the conclusion that some structures or large-amplitude spectral components existing in the hiss band, are able to phase-bunch the resonant electrons, then leading to the excitation of chorus emissions. The presence of wavelets in hiss band was later studied by TSUJI *et al.* (1989). However, it seems that the experimental data presented by KOONS (1981) are not so persuasive as to indicate that hiss is a source of chorus. Hence, more extensive experimental studies are highly desirable on his implication concerning the mechanism of hiss-triggered chorus, *i.e.* whether hiss is actually a source of chorus or not. For this purpose, the application of detailed signal analyses is of essential use.

The purpose of the present paper is to present detailed experimental findings on the cause and effect relationship between hiss and chorus, such as the role of hiss in the generation of chorus in the outer magnetosphere. The study is based on detailed spectral analyses and direction finding measurements for the VLF/ELF emission events indicating the simultaneous presence of hiss and chorus seeming to be closely correlated with each other. We examine similar emission events as studied by KOONS (1981), but our study is more sophisticated and more detailed than his work in the following respects. In his experiment the wave field was measured only by an electric antenna and the electron density was not unfortunately measured, although his results relied on a high level of density. On the other hand, in this paper, we make full use of a complete set of wave data observed onboard the GEOS 1 satellite. The application of detailed spectral analyses to the waveform data enables us to investigate the fine structures existing in the hiss band, and the simultaneous measurements of multiple field components make it possible for us to determine the wave normal directions of both hiss and chorus. In Section 2 we describe the data base obtained from the GEOS 1 satellite. Section 3 deals with the investigation of fine structures within the hiss band by means of two different kinds of spectral analyses, and in Section 4 we present results of direction finding for hiss and chorus. Finally, in Section 5 we summarize experimental findings obtained from this investigation and we discuss physical implications.

2. Data Source

The field data used are signals obtained by the so-called S-300 experiment on board the GEOS 1 satellite, which measures continuously the electric and magnetic components of the field by six antennas. The data are recorded by a swept frequency analyzer (SFA) system. Six SFA's operate as heterodyne systems controlled by a single frequency synthesizer. The analyzers select bands of 300 Hz in a frequency range 150 Hz to 77 kHz by steps of 300 Hz, thus giving a complete coverage. The transposed signals are sampled 1488 times per second (Nyquist frequency=744 Hz), and the high pass filter of the 300 Hz SFA band is positioned at 150 Hz and low pass filter at 450 Hz. See S-300 EXPERIMENTERS (1979) for more detailed description of the wave experiment onboard the GEOS 1.

The spectral analyses to find out fine structures of hiss emissions are based on waveform data of the SFA's. Furthermore, the spectral matrix composed of the auto-power and cross-power spectra among six field components at each Fourier frequency component is estimated by using SFA data in VLF part, and these are used for subsequent direction finding measurements to determine wave normal directions.

3. Wave Characteristics and Spectral Analyses of the Fine Structures of VLF/ELF Emissions

Wave data extensively used in the present study are obtained on the GEOS 1 satellite during the period of about 30 minutes from 1212: 42 to 1241: 11 UT on July 21, 1977, at L value of 6.5–6.7 around MLT$\simeq$13 h and at geomagnetic latitudes from 6.8°–8.5°. The K_p index at the time of observation was 2, but this emission event seems to be closely correlated with a severe magnetic disturbance about one day before, as shown in Fig. 1(a). We have also used an additional data set observed at relatively higher geomagnetic latitude (24.2°–23.6°) during the period of 0812: 00 to 0824: 03 UT on December 2, 1977. The L value for this part of orbit is 6.2$\sim$5.8 and MLT$\simeq$ 9 h, and the variation of K_p index for this event is also presented in Fig. 1(b). In the following we will describe characteristics of both hiss and chorus occurring simultaneously in order to discuss to the role of hiss in triggering chorus.

3.1. General characteristics of dynamic spectra

A few sonagrams in ELF band (0–2.5 kHz) observed by the b_X antenna are selected from the first near-equatorial event and they are illustrated in Fig. 2(a)–(d). The spectrograms in these figures are Fourier-transformed results of onboard-computed correlograms, and the alphabetical order (a→d) corresponds to the time progress. Especially below the spectrogram in Fig. 2(a), there are indicated four temporal variations (time resolution=86 ms) of emission magnetic field (b_X) intensity of emissions at the four specific frequencies (735, 918, 1010 and 1194 Hz, all with the same bandwidth of 92 Hz) in the same linear scale. The intensity variation at the lowest frequency of 735 Hz represents mainly the hiss component as understood from the above spectrogram, and those at the higher two frequencies (1010 and 1194 Hz) do the chorus component, while the intensity variation at 918 Hz seems to represent the boundary

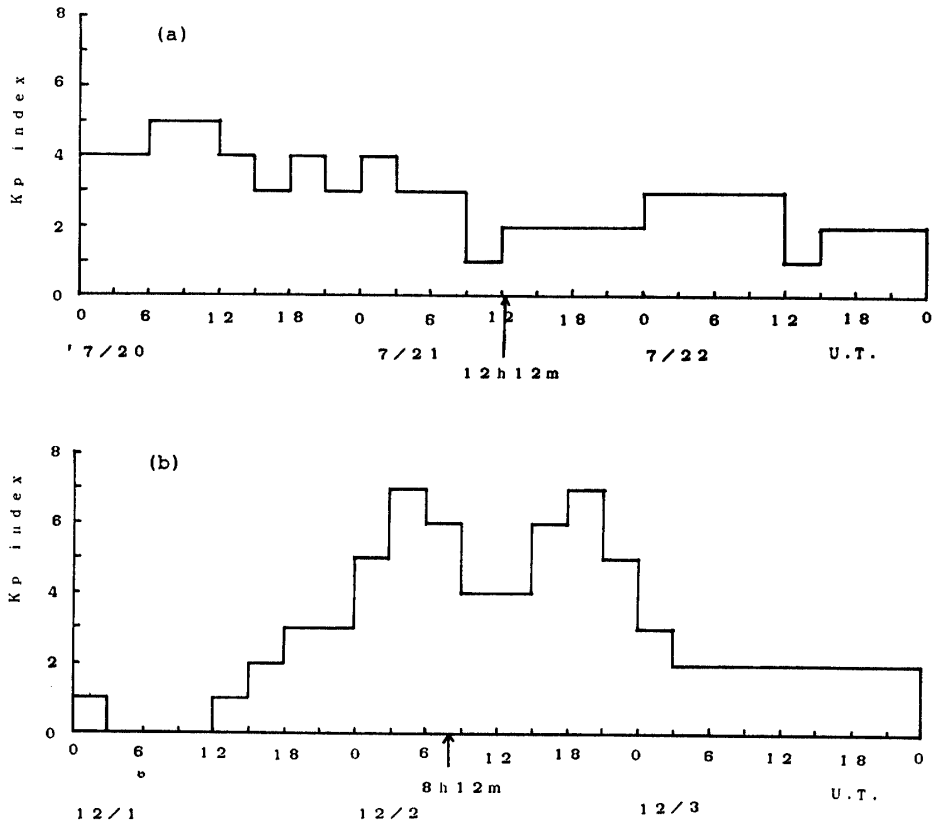

Fig. 1. The temporal variation of K_p index including the day when we observed hiss-triggered chorus. The arrow shows the time when the event was observed onboard satellite. (a) 20–22 July 1977 and (b) 1–3 December 1977.

between the hiss and chorus. Other three figures, Fig. 2(b)–(d) show temporal variations of the 735 Hz emission intensity which may reflect the hiss intensity in the same scale as Fig. 2(a) so that we can compare easily the hiss intensities in different figures. We comment here on the identification of the phenomenon. We have called the signal below ~900 Hz as the hiss, but it is not clear why this part of the signal must be the hiss because they do not show characteristics of the hiss such as structureless spectrum and unchanging intensity over several minutes. This band might be identified as 'banded chorus' as found by BURTIS and HELLIWELL (1969) because of vertical structures. However, on the basis of the detailed spectral analyses in Section 3.2. by using the waveform data, this band below 900 Hz is actually hiss, though its intensity remains nearly steady only for a few tens of seconds.

These figures provide us with the general characteristics of events studied. It is likely that each chorus element in every spectrogram is triggered from the top of the underlying hiss band and also that starts of every risers are asymptotic to the hiss band (*i.e.* initially they have very small df/dt values). This point will also be examined in detail in the next subsection. A comparison between different spectrograms in Fig. 1 suggests that chorus occurrence is enhanced only when the underlying hiss becomes intense. This point is also quantitatively investigated later. These general properties are also reconfirmed for the off-equatorial second emission event on Decem-

ber 2, 1977.

The emission band around 1.5 kHz in Fig. 2(b) is identified as the half-gyrofrequency VLF emission which is generated near the equator at frequency above one half the electron gyrofrequency (HAYAKAWA *et al.*, 1984; MUTO *et al.*, 1987).

3.2. *More detailed spectral analyses for hiss and chorus and fine structures of hiss band*

The extensive spectral analyses have been performed for the waveforms taken at output of the SFA's. For the first event of July 27, 1977, two steps of frequencies are swept; step 2($592 \leqq f \leqq 1336$ Hz) for which the transfer function is constant between 742 and 1042 Hz and step 3($888 \leqq f \leqq 1632$ Hz) for which the transfer function is constant between 1038 and 1338 Hz. As a spectral analysis method we have adopted the periodogram method (WELCH, 1967; LEFEUVRE *et al.*, 1981). This periodogram is a direct application of FFT (fast Fourier transform) on the signal, and in the following the resolution of this spectral analysis is 23.25 Hz in frequency and 43 ms in time. Results by this method are presented in the form of intensity contour maps, and several examples will be illustrated in this paper.

An inspection of Fig. 2 produced from the onboard correlator shows that some vertical structures are included even in spectra of the signal below ~900 Hz, and it may be considered that this part of the signal (we call it "hiss" in this paper) may be

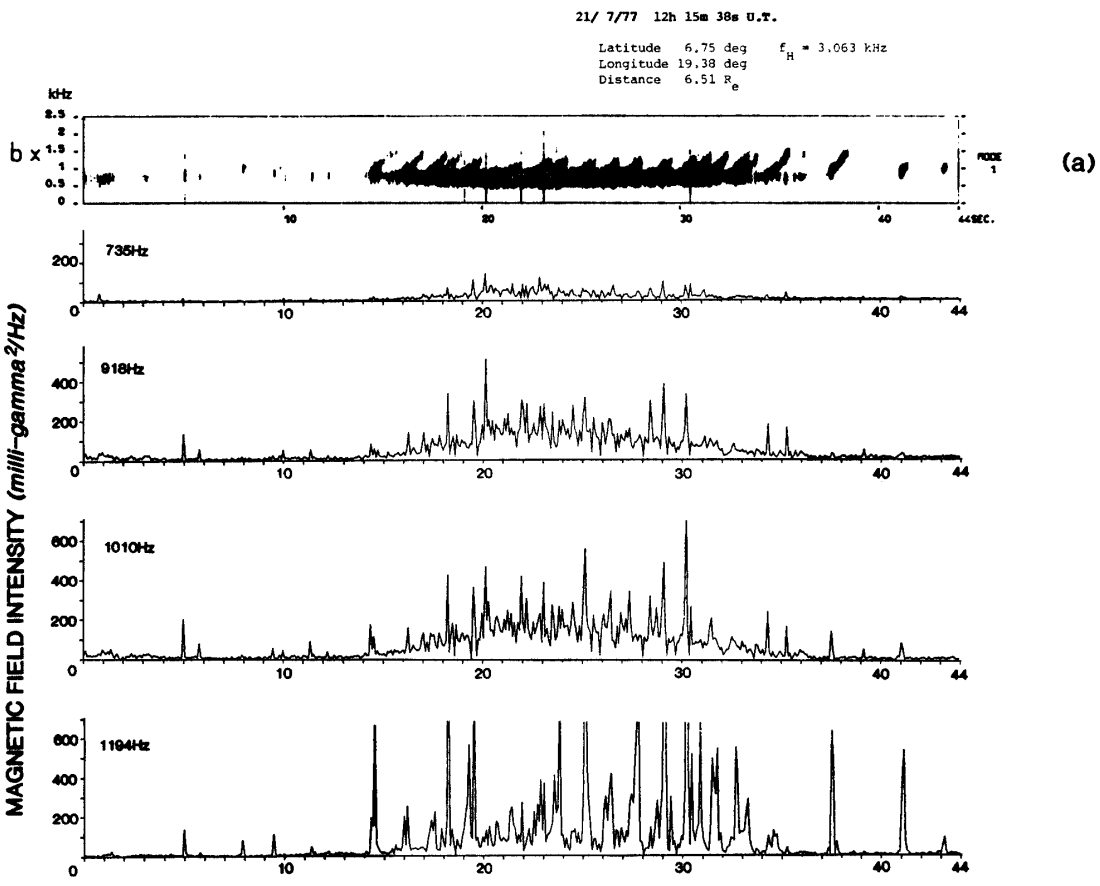

Fig. 2.

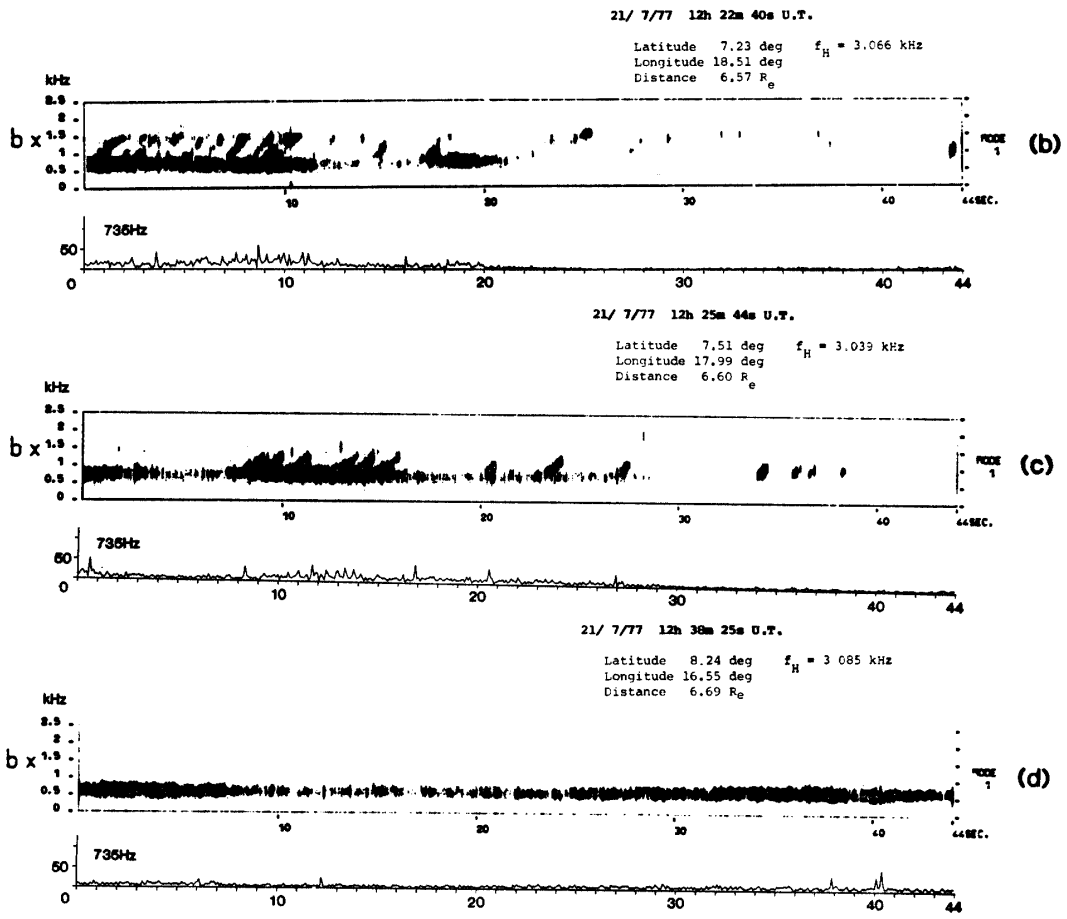

Fig. 2. The spectrograms of magnetic field (b_X component) observed onboard GEOS-1 satellite in the near-equatorial region on 21/7/1977. The alphabetical order (a)→(d) corresponds to the time progress. Below the spectrogram of figure (a) are illustrated the intensities at the four frequencies of 735, 918, 1010 and 1194 Hz. The component at 735 Hz refers to the intensity of hiss, that at 918 Hz means the intensity of the boundary between hiss and chorus, and the other two frequencies correspond to the intensity of chorus. Below the figures (b)–(d) is shown the temporal variation of the hiss component at 735 Hz alone.

seen like as "banded chorus" as pointed out by BURTIS and HELLIWELL (1969). However, these vertical structures confused with the "banded chorus", are clearly an artifact due to the signal analysis. The spectra of Fig. 2 have been obtained from Fourier transformation of the correlation functions produced by the onboard correlator. Since the correlator is operated in time sharing (autocorrelogram on one component, autocorrelogram on the other component, *etc.*), we get time intervals with zero values. This results in vertical structures; this point is easily checked by performing a spectral analysis on the waveforms transmitted onto the ground, and the spectrograms obtained over the same time intervals have not such vertical bar structures (See Figs. 3 and 4. These contour maps are drawn by using the same waveform data, and we cannot find out any vertical structure in hiss band). A double-check has been made by carrying out the stationarity tests (BENDAT and PIERSOL, 1971; LEFEUVRE and PARROT, 1979) on the data of Fig. 2. Signals of the hiss part are stationary in

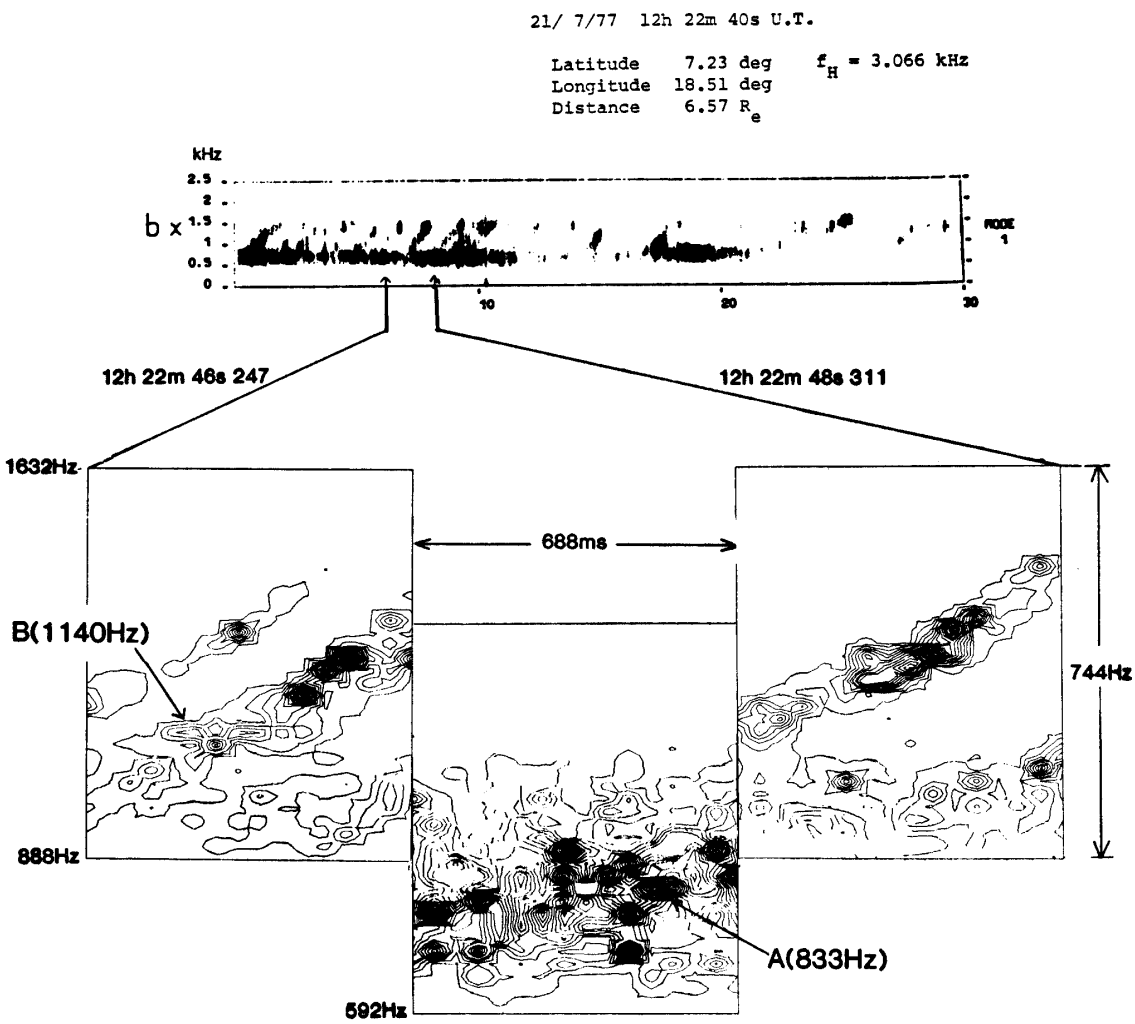

Fig. 3. The results of the detailed spectral analyses during 1222: 46 247 ms–1222: 48 311 ms UT in Fig. 2(b). This analysis was done with $\Delta t = 43$ ms and $\Delta f = 23.25$ Hz. Coherent wavelets with duration of $\geqq 100$ ms can be seen in the hiss band in the middle of the bottom contour map, and an example is marked by A.

time with a high confidence, and the emissions below ~900 Hz are definitely the hiss. On the same reasoning, discrete emissions at frequency above ~1.0 kHz (we call them "chorus" in this paper) are also seen with vertical structures, but these vertical elements are again due to the artifact of signal analysis. Hence, the emissions above the hiss band are really chorus.

KOONS (1981) has suggested wavelets in a hiss band based on the simple FFT analysis for very limited data. Then, recently TSUJI *et al.* (1989) have made spectral analyses for both a ground-based hiss without accompanying any chorus and a white noise from a random noise generator by means of different methods as adopted in this paper, and they have found that wavelets are confirmed only in the hiss band and that no such wavelets are noticed in the white noise. This point will be important for discussing the hiss and chorus shown in Fig. 2.

Figure 3 illustrates and example of spectral analyses by the above analysis method for an interval (three successive time intervals with each interval of 688 ms) selected

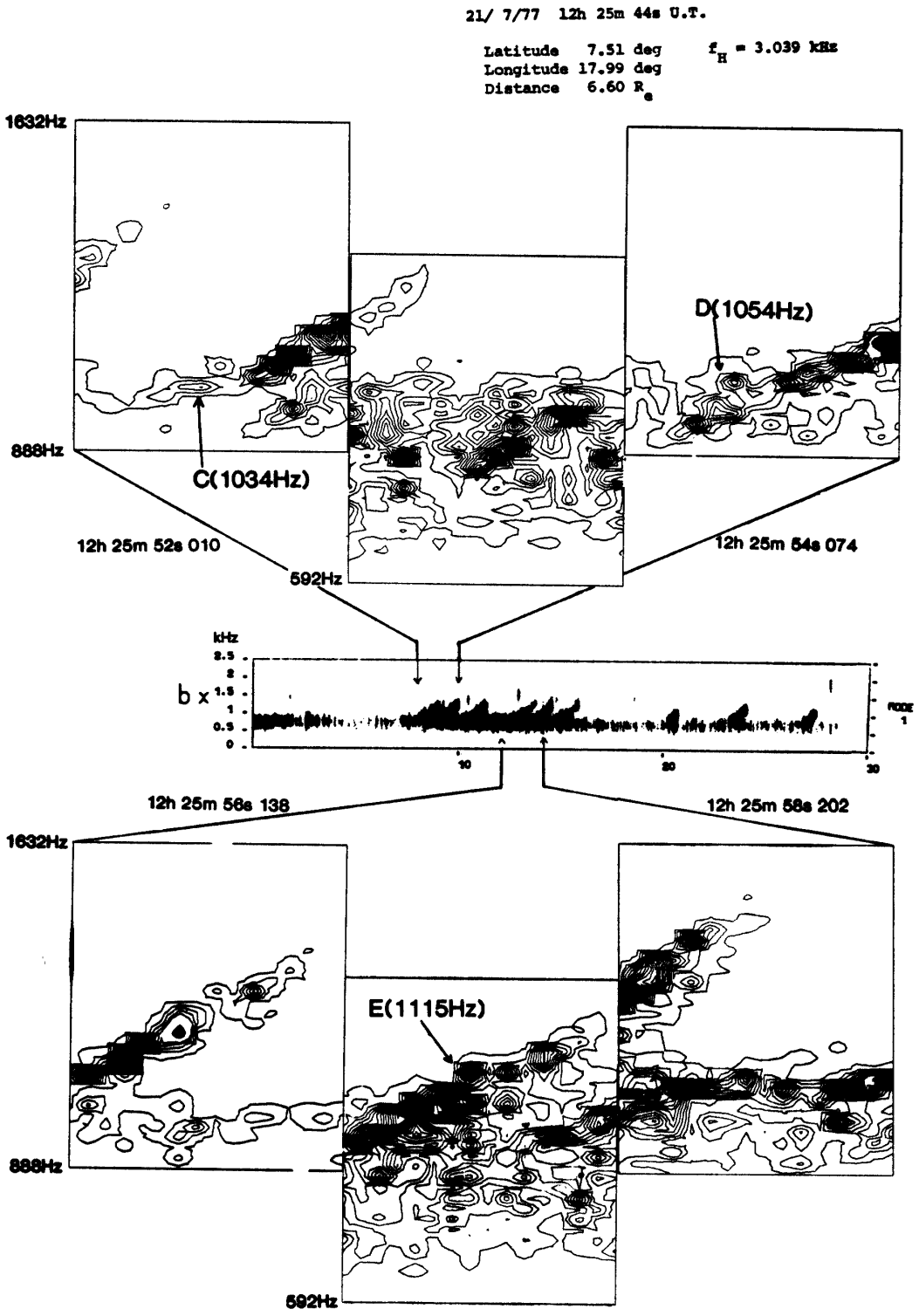

Fig. 4. The intensity contour maps during 1225: 52 010 ms–1225: 54 074 ms UT and 1225: 56 138 ms–1225: 58 202 ms UT in Fig. 2(c). There are also some wavelets in the hiss band. Among them we select the wavelets which exist at the foot of the chorus element and labeled C–E. These wavelets may be considered to be the origins of the relevant chorus emissions.

from Fig. 2(b), and similar results for the two time intervals (starting at 1225: 52 010 ms and 1225: 56 138 ms) in Fig. 2(c) are presented in Fig. 4. In contour maps in Figs. 3 and 4, the amplitudes in each 688 ms time interval are normalized by the maximum intensity. Then, we plot contour lines between a minimum value of 0.02 and a maximum value of 1.0, and an increment between successive contours is 0.04. In particular, the middle of bottom panels of Fig. 3 indicates a very random nature of the hiss band. However, we can find out some structures in some parts of the hiss band; that is, we can find island structures in contour maps, and a few examples can be selected in Figs. 3 and 4. We notice good examples of a monochromatic wave component (or a wavelet) with duration of about 100–200 ms at a given frequency in the hiss band. For example, we can find out a wavelet with duration of about 100 ms at a frequency of about 833 Hz, which is indicated by A in the middle of the bottom panel of Fig. 3. Similar wavelets with the same order of duration in the hiss band are also found in other figures. Although we see in spectrograms that the hiss appears at frequencies below $\sim$900 Hz, the contour maps show that the hiss band extends even up to 1000 Hz. Hence, we cannot point out the boundary between the hiss and chorus clearly, but we can safely say or confirm again from these contour maps that each chorus element is asymptotic to the upper edge of the hiss band. The same signal analyses have also been carried out for the second event on December 2, 1977, and its result is illustrated by contour plots in Fig. 5. Again, it is easy for us to find some wavelets in the hiss band, especially in the right bottom panel. Hence, the suggestion by KOONS (1981) for very limited data and by TSUJI *et al.* (1989) for the ground-based hiss data on the presence of wavelets within the hiss band is also confirmed by this study.

Results by the above spectral analysis have been checked by using another vectorial A.R. (auto-regressive) method (LAGOUTTE and LEFEUVRE, 1985) for which the same temporal resolution of 43 ms is adopted, but the frequency resolution can be made as small as possible. Six Hz is temporally used as the frequency resolution, and results through the second method support those by the previous method, although the latter is not shown in the present paper.

Next, we investigate experimentally whether these wavelets near the upper edge of the hiss band trigger chorus emissions. The spectrograms in Fig. 2 have suggested that chorus elements are triggered by the hiss band, and we examine the detailed spectral analysis in Figs. 3, 4 and 5 with paying particular attention to the foot part of each chorus element. We notice examples of a wavelet with duration about 200 ms at a frequency around 1140 Hz indicated by B in the first bottom panel in Fig. 3 and similar wavelets at a frequency of 1034 Hz indicated by C in the upper first panel, at a frequency of 1054 Hz indicated by D in the upper last panel and at a frequency of 1115 Hz indicated by E in the middle of the bottom panel in Fig. 4. In these examples of the near-equatorial event in Figs. 3 and 4, the best example for the association of a wavelet with a chorus element is shown by the first top panel in Fig. 4. A wavelet at the frequency of 1034 Hz (indicated by C) seems to be the origin of the chorus, because it is located exactly at the foot of the relevant chorus element. Then, in the middle bottom panel of Fig. 4, it is clear that there are some internal structures at the part of the hiss where the chorus element is asymptotic to, but it seems difficult to say which wavelet is the origin of the chorus element. Further good examples are

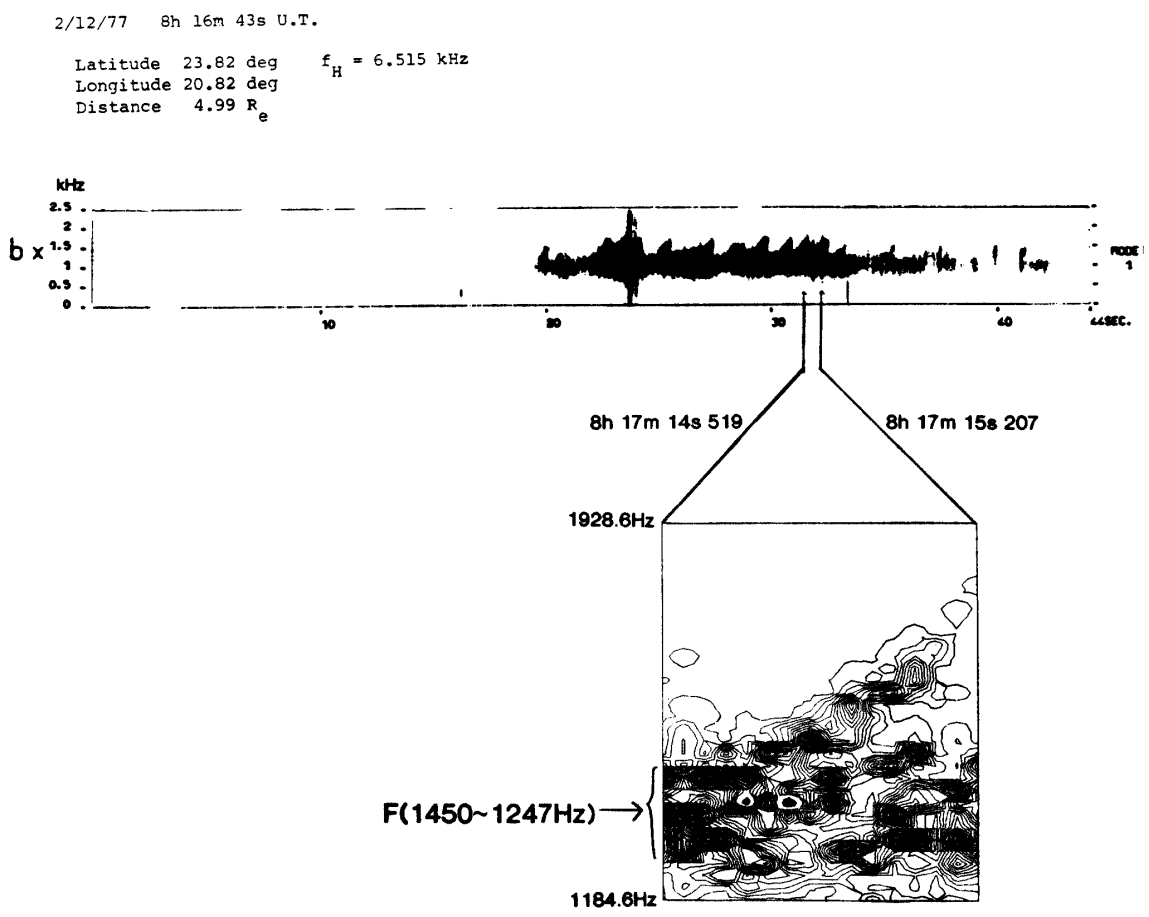

Fig. 5. The intensity contour map for the off-equatorial observation onboard GEOS-1 satellite. We confirm that there are some wavelets with duration of 100 ms or more in the hiss band, and a group of wavelets indicated by F are seen at the foot of a chorus element.

readily identified in the both panels from the off-equatorial event in Fig. 5. The chorus element is accompanied by a conspicuous group of wavelets (indicated by F) at the frequency of 1450–1247 Hz at the foot of the chorus whose duration is of the order of 200 ms. In this case the chorus element is smoothly extended from one of the wavelets indicated by F. However, one may notice a gap between the chorus element and the corresponding wavelet deeming to be its origin for the cases such as C, D and E, and we will discuss this effect in Section 4.

The frequency drift rates of chorus elements (df/dt) can be investigated by using the spectral analyses as in Figs. 3, 4 and 5. It is found that the df/dt's of the chorus elements are about 0.7 kHz/s when we approximate the chorus element above the hiss band by a linear line, and these values are considered to be consistent with those by KOONS (1981). But as for the off-equatorial event, the df/dt values of chorus elements are very scattered between 0.4–1.3 kHz/s and the df/dt in Fig. 4 is accidentally the same value as in the case of the equatorial event.

3.3. *Relationship of the intensity and occurrence of chorus elements with those of the hiss band*

A close correlation between the hiss intensity and chorus occurrence as inferred in Fig. 2 is more quantitatively investigated by comparing the intensity and occurrence rate of chorus elements with respect to those of hiss. Intensities at the four frequencies of 735, 918, 1010 and 1194 Hz measured every 86 ms are already plotted in Fig. 2(a), and we use magnetic field intensities at these frequencies. Furthermore, there magnetic field components (b_X, b_Y and b_Z) and an electric field (E_Y) are utilized. Signals at 735 Hz are attributed to the hiss in the near-equatorial event and this frequency is always below the foot of the chorus elements, while the higher two frequencies of 1010 and 1194 Hz correspond to the chorus from the sonagram. On the contrary, the signal at 918 Hz represents contributions from both the hiss and chorus. Correlations for every combinations among the four frequencies are investigated, and Fig. 6 shows an example of a scatter plot between the simultaneous intensities of hiss intensity at 735 Hz and the chorus intensity at 1010 Hz at every 86 ms for the time interval of Fig. 2(a) measured by the b_X antenna. If we assume, as mentioned before, that a wavelet near the upper edge of the hiss band is responsible for a chorus element, we must investigate the correlation of chorus intensity with that of hiss slightly ahead of the chorus, but this kind of study seems to be useless, because as shown before it is sometimes difficult to identify the association of the causative wavelet with the chorus, and furthermore the temporal resolution of 86 ms used in this paper seems to be insufficient. Nevertheless, Fig. 6 based on the comparison of the intensities of hiss and chorus at the same time, is still useful to show the association of hiss with chorus. Figure 6 implies clearly a good correlation between the chorus and hiss intensities and the correlation coefficient in Fig. 6 is as high as 0.74. This experimental fact indicates strongly that the chorus intensity is very much influenced by the hiss intensity. The intensity ratios at these two frequencies are studied for all events (a)–(d) in Fig. 2, and it is then found that the chorus power is about 6 dB higher than the hiss power. However, the intensities at the higher two frequencies of 1010 and 1194 Hz are nearly the same.

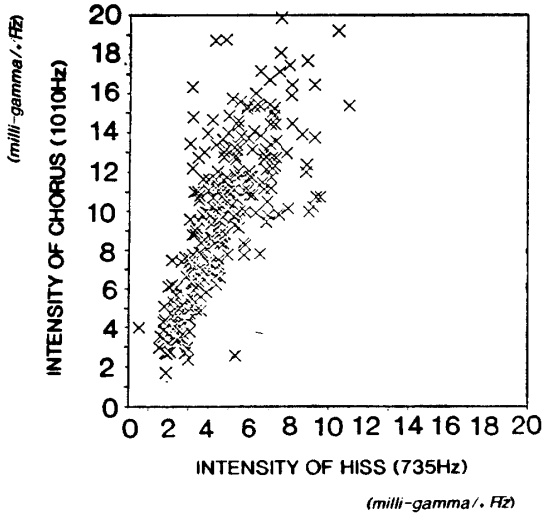

Fig. 6. The relationship of magnetic field intensity of hiss (735 Hz) and that of chorus (1010 Hz) for the event of Fig. 2(a).

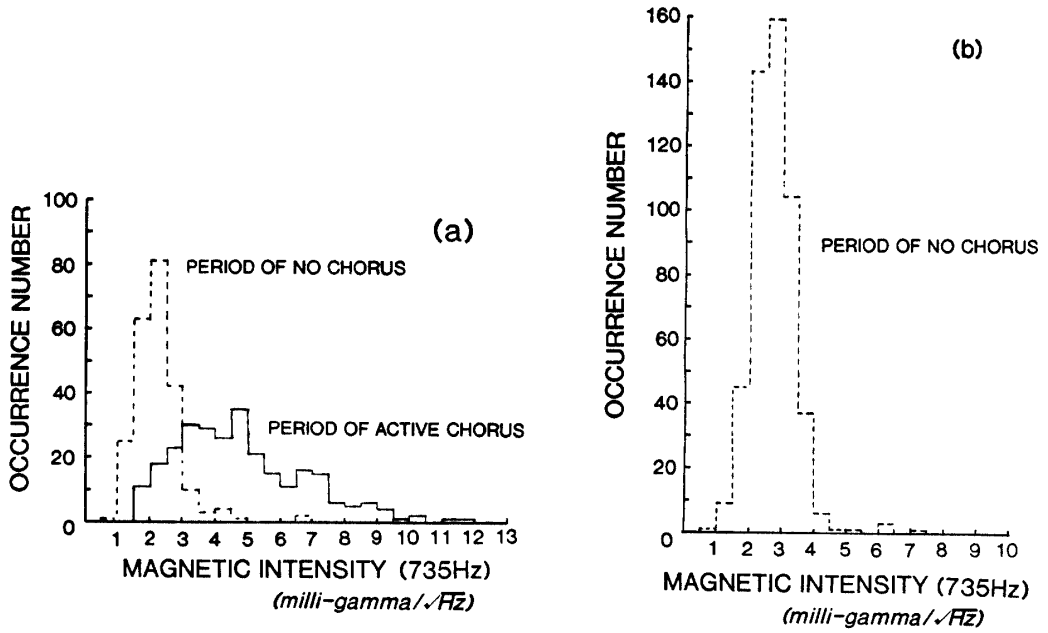

Fig. 7. The occurrence histogram of the magnetic field intensity of hiss (735 Hz). (a) indicates the result of Fig. 2(a) and a full line refers to the period of active chorus and a broken line corresponds to the period of inactive chorus. (b) shows the case of no chorus period of Fig. 2(d).

It can be easily supposed that very low intensities at 1010 Hz in Fig. 6 imply the absence of chorus or the background noise. Therefore, we have plotted, in Fig. 7(a), the occurrence histograms of the hiss intensity (735 Hz) when we are in the period of high chorus activity (in a full line), and also in the inactive chorus period (in a broken line). The criterion between the period of active chorus and of no chorus is a little bit subjectively estimated in the spectrogram of Fig. 2(a). For example, the main active period is taken as the interval from 1215: 52 751 ms to 1216: 13 821 ms, and the other interval corresponds to that of no chorus activity. The magnetic field intensity of hiss during the period of no chorus indicated by a broken line, is found to be well peaked from $1m\gamma/\sqrt{Hz}$ to $3m\gamma/\sqrt{Hz}$, with a weak tail up to $7m\gamma/\sqrt{Hz}$. On the other hand, the hiss intensity at 735 Hz during the active chorus period exhibits a broad maximum with intensity range from $1.5m\gamma/\sqrt{Hz}$ and to $12m\gamma/\sqrt{Hz}$. By comparing these two intensities and by considering our crude criterion on the chorus activity, the hiss intensity is likely to be above a few $m\gamma/\sqrt{Hz}$ for an active chorus occurrence, this value being a threshold value of the hiss intensity for the excitation of chorus. A similar histogram of the hiss intensity for the case of Fig. 2(d) in which no chorus takes place, is illustrated in Fig. 7(b). The histogram in broken line extends up to about $4m\gamma/\sqrt{Hz}$, and this further support the previous threshold hiss intensity, a few $m\gamma/\sqrt{Hz}$ for exciting a chorus.

A figure corresponding to Fig. 7 is illustrated in Fig. 8 for the off-equatorial event on December 2, 1977. Probably because of the propagation effect toward a high geomagnetic latitude, it might have obscured such a clear separation between the full and broken lines as found in Fig. 7(a). However, it would be safe to say again that the threshold for exciting a chorus for the off-equatorial case is about a few $m\gamma/\sqrt{Hz}$,

which is consistent with that for the equatorial event.

The above analyses are statistical, and all the intensities of wavelets indicated by alphabets in Figs. 3 and 4, are found to be above $5m\gamma/\sqrt{Hz}$. The wavelet B is about $5.1m\gamma/\sqrt{Hz}$ at its peak intensity. The wavelet C which is another good example of the association with the resultant chorus, has a peak intensity of about $6.6m\gamma/\sqrt{Hz}$.

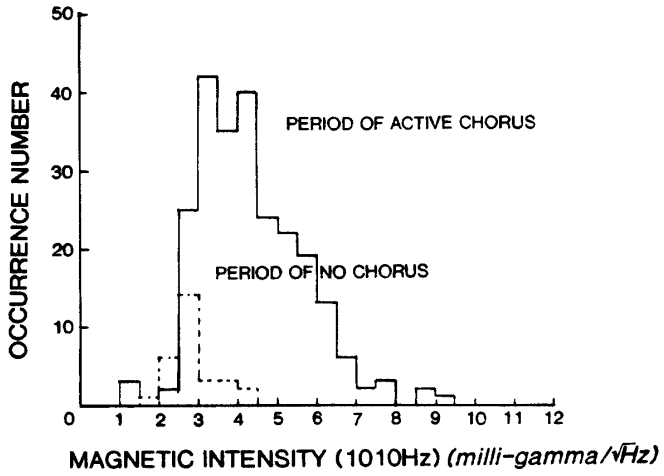

Fig. 8. The same as Fig. 7, but for the off-equatorial event on December 2, 1977.

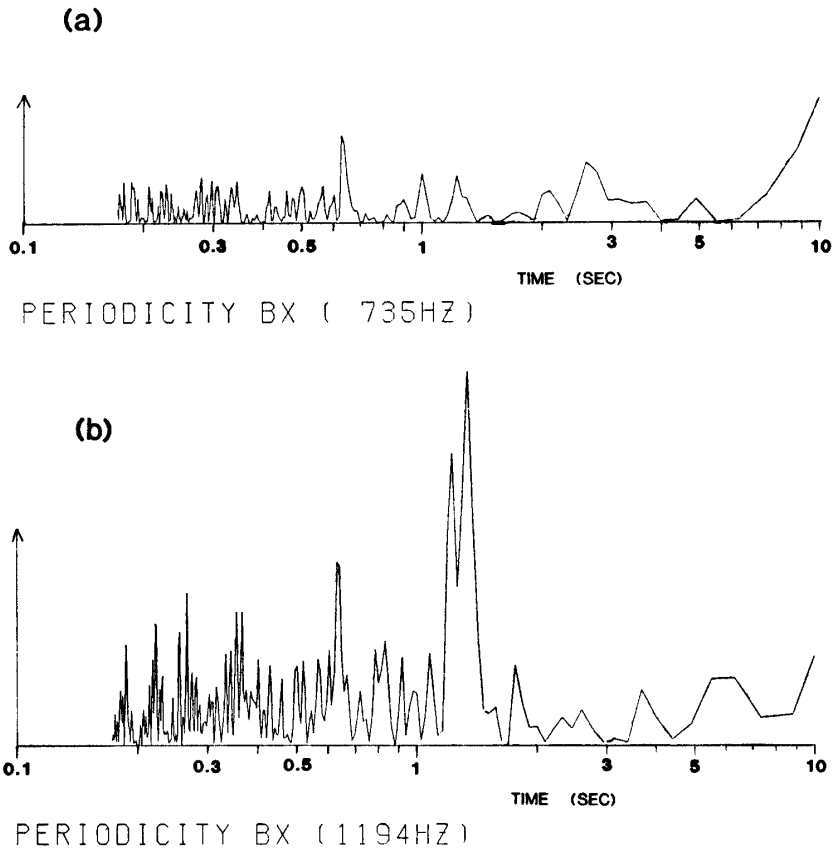

Fig. 9. The periodicity of the hiss magnetic field intensity (735 Hz). (a) corresponds to the result for Fig. 2(b) and (b) indicates the result for the off-equatorial observation.

Finaily, it is found that other wavelets D and E have an intensity of 9.3 and 15.5m$\gamma/\sqrt{\text{Hz}}$, respectively. The average intensity of wavelets indicated by F is found to exceed the threshold value.

3.4. Harmonic analysis for chorus and hiss

Figure 9(a) illustrates a power spectrum of the time series data of the hiss intensity at 735 Hz, and Fig. 9(b) indicates the same analysis at 1194 Hz corresponding to chorus. The data of Fig. 9 are based on the event of Fig. 2(a) observed by the b_x antenna. Figure 9(a) indicates that there are no remarkable periodicities in the hiss intensity at 735 Hz, although we have already known in Section 3.2 that there are several wavelets in the hiss band on several occasions. Then, it is considered that such wavelets occur very irregularly and spontaneously even if they exist. On the contrary, the chorus intensity in Fig. 9(b) exhibits a noticeable periodicity around 1.3 s, though two closely spaced peaks are present. However, this period seems to have no connection with the 2-hop whistler-mode group delay of 4.0–5.0 s (M. TIXIER, private commun.) as found in periodic emission, and the reason of this periodicity is unknown at the moment. The same harmonic analyses have been made for the second off-equatorial event on December 2, 1977, and we have again found a periodicity of about 3.0 s which is different from that for the first event.

3.5. Wave normal directions of hiss and chorus

Figure 10 illustrates an example of the computer display on the measurement of wave normal directions (θ, ϕ) of VLF emissions (both hiss and chorus), where θ is the angle between the wave normal and Earth's magnetic field and ϕ is the azimuthal angle measured from the magnetic meridian plane as defined in LEFEUVRE *et al.* (1981) and HAYAKAWA *et al.* (1984, 1986a). 688 ms (=43 ms (one time division) $\times$64 time divisions) is taken as a unit time interval as seen in Fig. 10, and one frequency division means 23.25 Hz in Fig. 10. The same analyses have been carried out for successive time intervals. The determination of wave normal directions of emissions is based on MEANS' (1972) method assuming a single plane wave and we use only three magnetic field components in obtaining Fig. 10. The numerics in the θ plot on the left half indicates the following values; 1 indicates $0^\circ \leqq \theta < 10^\circ$, 2, $10^\circ \leqq \theta < 20^\circ$ and so on. Similarly, in the ϕ plot on the right half, 1 indicates $0^\circ \leqq \phi < 45^\circ$, 2, $45^\circ \leqq \phi < 90^\circ$ and so on. The direction findings have been carried out only for signal intensity above the prescribed threshold. We can identify two chorus elements even for the direction finding results in Fig. 10. We have to comment on the usage of MEANS' method. This method is applicable and very suitable for rather structured emissions such as chorus, and so there involves no problem in the results of (θ, ϕ) for the parts of chorus elements. However, an application of this method to unstructured noise like the hiss is questionable, and the wave distribution function method (LEFEUVRE *et al.*, 1981, 1982; HAYAKAWA *et al.*, 1986a, 1990; PARROT and LEFEUVRE, 1986) is suitable for such hiss emissions composed of infinitesimally small plane waves with no phase coherence. Figure 11 indicates an example of the results for chorus by means of these two methods, where $\times$ indicates the result by MEANS' method; we see that the peak of the wave distribution function ($\cdot$) is very consistent with MEANS' result. We have also used

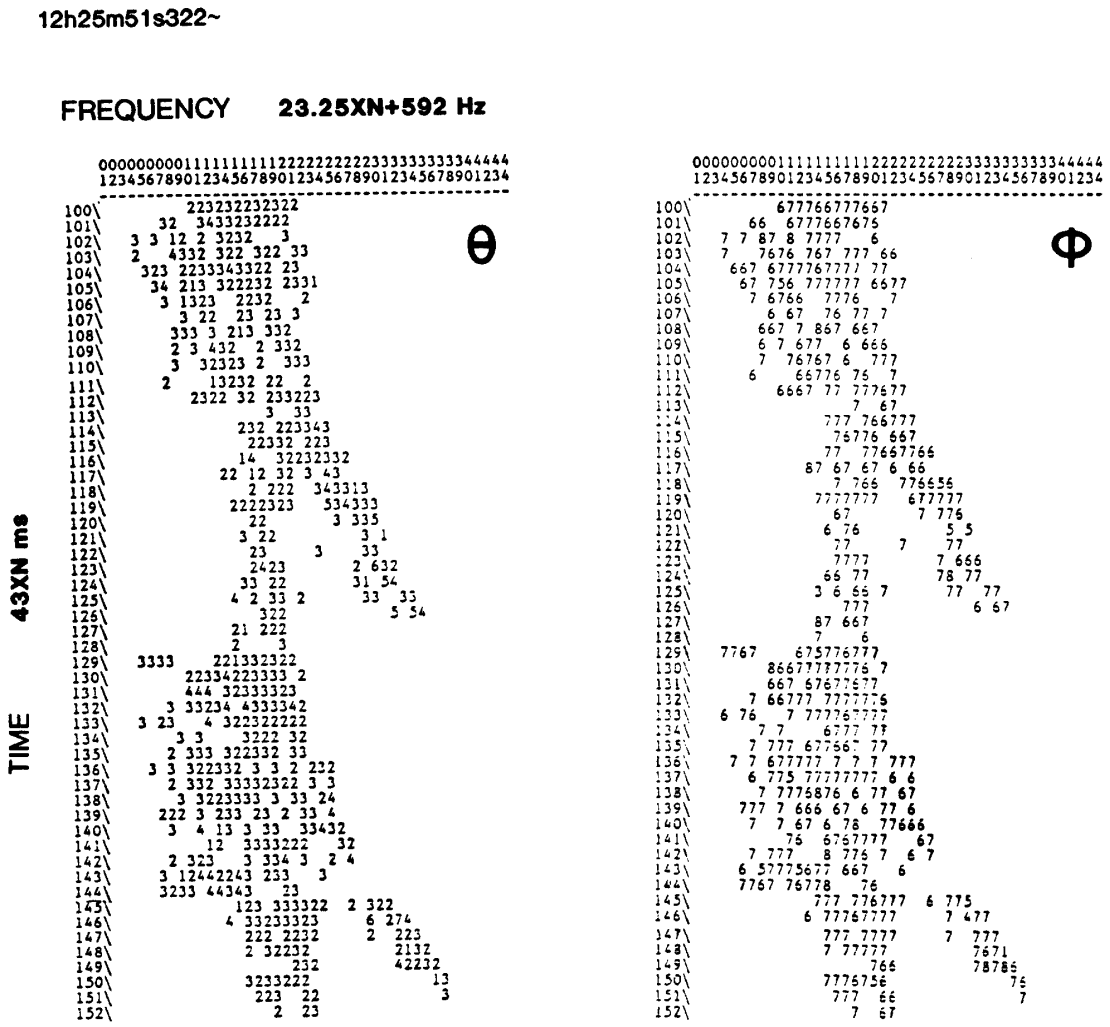

Fig. 10. An example of the direction finding results by MEANS' *method. This is the result of the part of Fig. 2(c) and the wave normal direction θ, corresponding to the polar angle, and the azimuthal angle ϕ are shown as the range numbers. As for θ, the range number 1 denotes $0° \leqq \theta < 10°$, 2 means $10° \leqq \theta < 20°$, and so on. As for ϕ, the range number denotes the value in every 45°, for example, the range number 1 indicates $0° \leqq \phi < 45°$.*

MEANS' method to the part of hiss and we have confirmed that the results of (θ, ϕ) by the wave distribution function and MEANS' method are very identical to each other as seen from an example in Fig. 12. This point was already confirmed by HAYAKAWA *et al.* (1986a).

Based on the computer plots as in Fig. 10, Fig. 13 summarizes the occurrence histograms of θ and ϕ for 11 seconds starting at 1222: 43 495 ms UT in Fig. 2(b), and the corresponding figures are illustrated in Fig. 14 for same 11 seconds starting at 1225: 51 322 ms UT as in Fig. 2(c). In both figures, full lines refer to the frequency range below 800 Hz, and broken lines above 1000 Hz. As seen from the sepctrograms in Fig. 2, 900 Hz is the upper edge of the hiss band and the signals around this frequency are combination of hiss and chorus. Actually, taking account of the contour maps (Figs. 3 and 4), there are some ambiguity for the boundary between hiss and

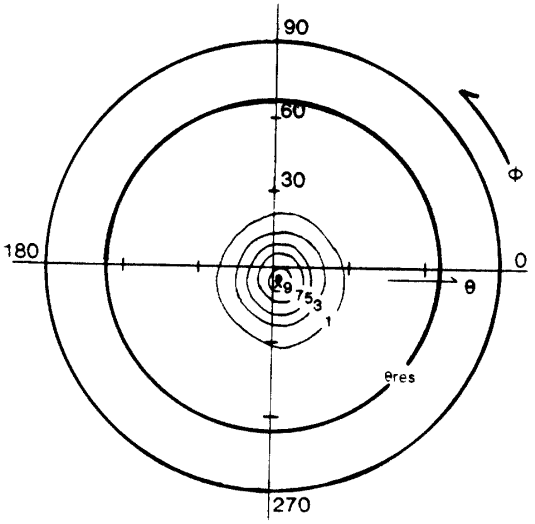

Fig. 11. An example of the wave distribution function for near-equatorial chorus at a frequency of 1167.48 Hz. The peak of the wave distribution function is indicated by •, which is found to be very consistent with MEANS' result given by ×.

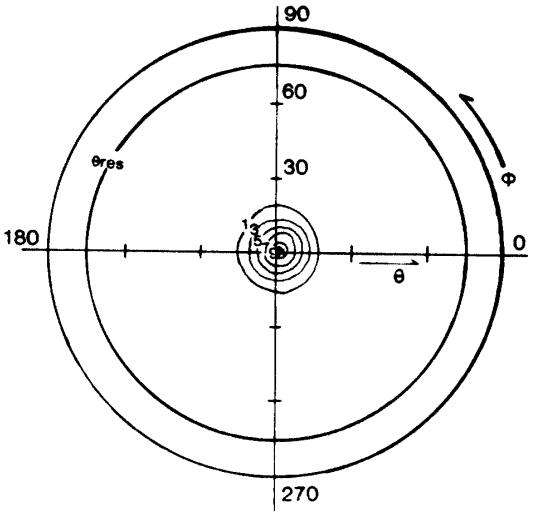

Fig. 12. The same as Fig. 11, but for the hiss at the frequency of 731.82 Hz.

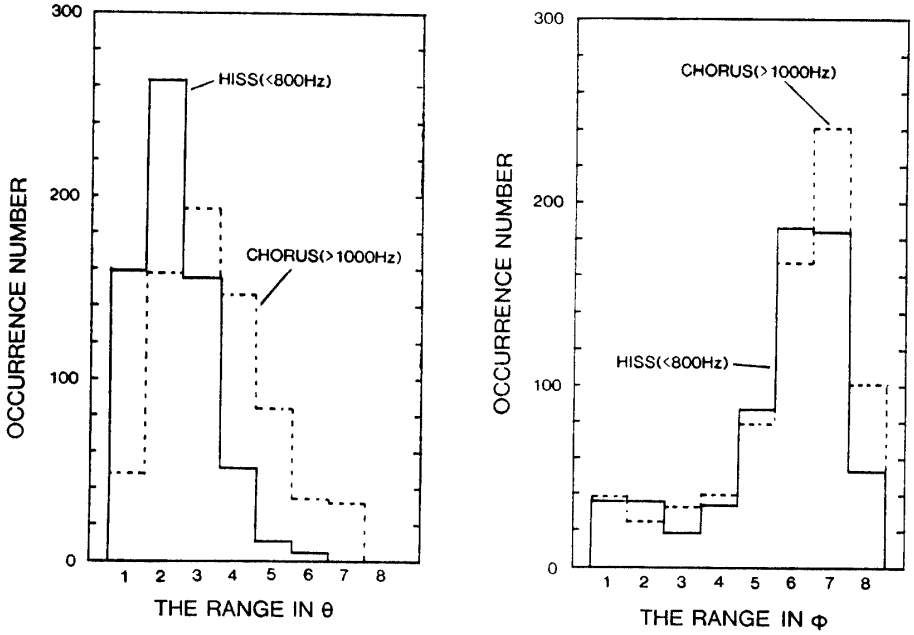

Fig. 13. The occurrence histograms of wave normal directions, θ and φ values, for 11 seconds starting at 1222: 43 495 ms UT in Fig. 2(b). Full lines refer to the frequency range below 800 Hz (hiss) and broken lines, the frequency range above 1000 Hz (mainly chorus).

chorus. In order to avoid this ambiguity, we have selected the above two frequencies, and so we assume the frequency range below 800 Hz as the hiss and above 1000 Hz as the chorus. The most important point in Fig. 13 is that we have very similar distributions in the azimuthal angle (ϕ) of the wave normal direction for both hiss and

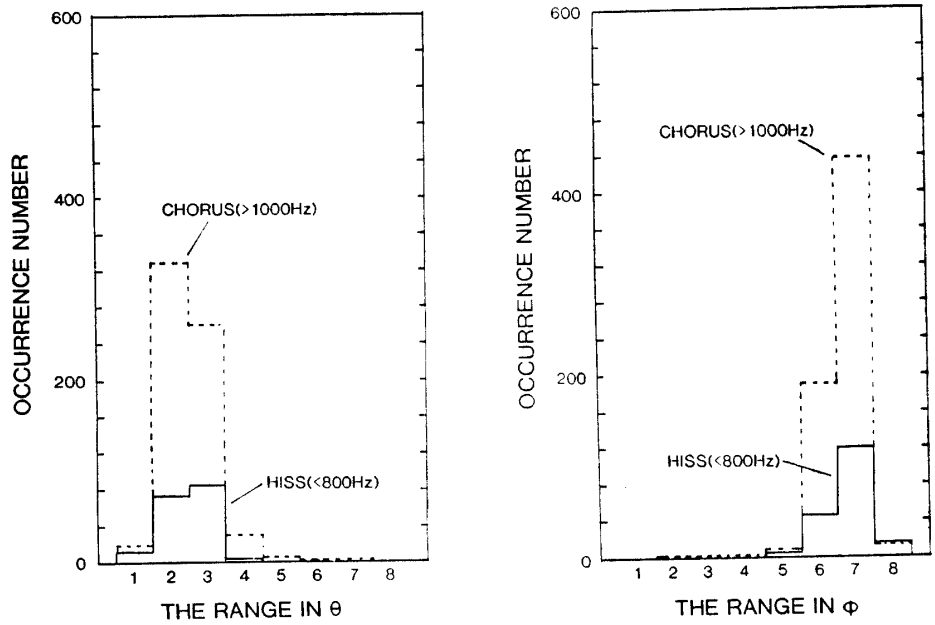

Fig. 14. The occurrence histograms of wave normal directions, θ and ϕ values, for 11 seconds starting at 1225: 51 322 ms UT in Fig. 2(c). Full lines refer to the frequency range below 800 Hz (hiss) and broken lines, the frequency range above 1000 Hz (mainly chorus).

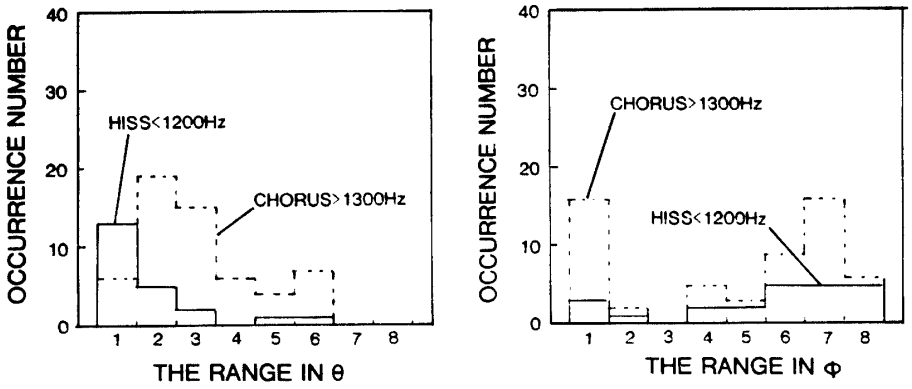

Fig. 15. The same as Figs. 13 and 14, but for the off-equatorial event.

chorus, and this is a strong indication that both phenomena come from the same source. On the contrary, we have found that the distributions in θ are different for hiss and chorus. That is, the θ distribution for the hiss is considerably broad, but smaller θ values less than 40° are common, whereas the chorus seems to have θ values slightly larger by about 10° than those for the hiss.

As already mentioned we have used only three magnetic field components and so there exists an ambiguity of 180° in propagation direction. In order to eliminate this ambiguity, we have also included one electric component (E_y) for every events, and then it is found that both chorus and hiss come from the equator.

The same analyses are performed for the event in Fig. 2(c) and the corresponding results are presented in Fig. 14. The θ's for the hiss illustrated by a full line are well concentrated to $\theta = 10°$–$30°$, and a very similar distribution in θ is noticed even for the

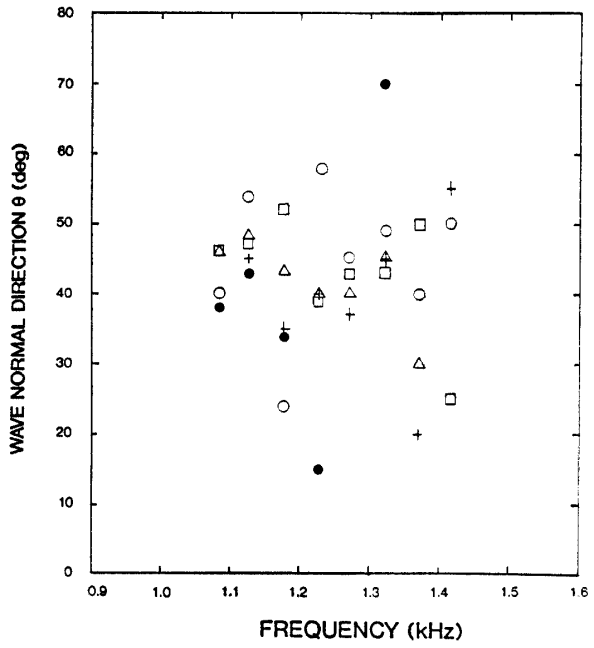

Fig. 16. The frequency dependence of wave normal angle θ of chorus elements during the period of Fig. 13. There are five elements indicated by different symbols.

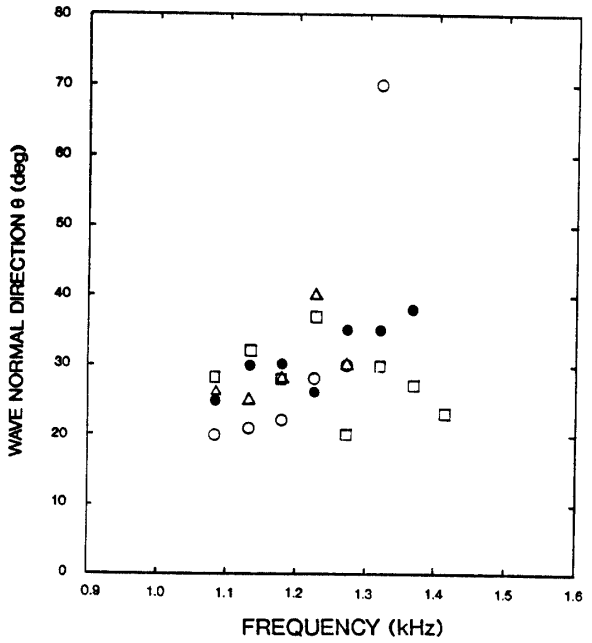

Fig. 17. The frequency dependence of wave normal angle θ of chorus elements during the period of Fig. 14. There are four elements indicated by different symbols.

chorus shown with a broken line. This point is a little bit different from the previous case. However, we have reconfirmed similar distributions in ϕ for both hiss and chorus.

The corresponding direction finding results for the off-equatorial event on December 2, 1977, are summarized in Fig. 15. Again, MEANS' method was adopted. The

most important point from this off-equatorial event study is that the distributions in ϕ for both hiss and chorus are again very similar to each other, although we notice a significant difference in θ distribution for the both phenomena.

The above information on the wave normal directions of VLF emissions is statistical, and we cannot study the frequency dependence of the wave normal direction for each chorus element. Figure 16 illustrates the frequency dependence of the wave normal angle (θ) of chorus elements during the period of Fig. 13. Five elements are indicated by different marks. This figure indicates that there seems to exist no specific dependence of the θ value for each chorus element on frequency. Then, Fig. 17 corresponds to Fig. 14, and four chorus elements are analyzed. It appears that θ increases with increasing frequency for this analysis period, except for a chorus element indicated by a square. Although not shown in this paper, we have to add that the ϕ value for each chorus element is nearly the same. From these direction finding results for ϕ, we can conclude that hiss and chorus came from the same source region.

4. Summary of Experimental Studies and Discussion

Based on the spectral analyses and direction finding measurements for hiss and chorus observed simultaneously near and far away from the geomagnetic equator in the outer magnetosphere by the GEOS-1 satellite, the following are the summary of the observational facts which are important for the study of the role of hiss in triggering chorus or not.

(1) The spectrogram by means of the correlators and also the spectral analyses have reconfirmed that each chorus element seems to be originated from the underlying hiss. Each chorus trace is asymptotic to the hiss band and that the df/dt at the foot of each chorus is nearly zero, and the frequency drift rate of chorus elements near the equator is about 0.7 kHz/s, as observed so far.

(2) The intensity and occurrence of chorus emissions are closely correlated with the intensity of the underlying hiss band. When the intensity of the underlying hiss exceeds a threshold value of a few $m\gamma/\sqrt{\text{Hz}}$, the excitation of chorus emissions is enhanced.

(3) The spectral analyses have established that hiss is, on some occasions, very random and incoherent, but that some parts of hiss exhibit wavelets (*i.e.* monochromatic wave component with duration of 100 ms or more). We can identify, on some occasions, wavelets at the foot of some chorus elements which may trigger chorus emissions, but on the other occasions the association of the causative wavelet with the chorus is not clearly identified.

(4) The most important new direction finding fact about the association between hiss and chorus is that the same ϕ values are obtained for hiss and chorus. This implies that the both phenomena of hiss and chorus come from the same source region. The hiss emissions propagate with small wave normal angles, less than 30°, but the wave normal directions (θ) of chorus emissions exhibit different behaviours for different events. Some chorus emissions propagate with small wave normal angles, but other chorus emissions have large θ values.

(5) The θ values for some chorus elements increase with increasing frequency,

but other chorus elements have no definite dependence of θ on frequency.

(6) There exists a periodcity in the occurrence of chorus triggered by hiss.

Based on these experimental findings (Items (1), (2) and (3)), we briefly discuss the main point of this paper; the possible association between hiss and chorus. TSUJI *et al.* (1989) have performed the detailed spectral analyses (as adopted in this paper) to the white noise from a random noise generator. The results are compared with the spectral analyses for the natural hiss without accompanying chorus. There have been no wavelets in the white noise, but some wavelets in the hiss and the presence of wavelets within the hiss is confirmed by extensive spectral analyses. Then, we have obtained a few good examples of the possible association between the causative wavelet and the chorus. However, this association was not always so persuasive, and even in this case there were always a few possible wavelets which may be causative to the relevant chorus element. Since in some cases there seems to exist an intensity gap between a causative wavelet and a chorus deeming resultant in Figs. 3, 4 and 5, one may suppose that the association between the two is inconvincing. However, even in the case of transmission experiments from Siple, the transition from the transmitting signal to the triggered signal is not so smooth on the basis of narrow-band spectral analyses (SA, 1990) such that he finds fine structures (or intensity variations) in the triggered emissions. Hence, the presence of such an intensity gap between a wavelet and a chorus for some cases is not considered to deny the association between the two. The reason for such gaps is not known at present, but we can list the following possibilities. SA (1990) has indicated that the main features of triggered emissions are that the transmitted waves grow, shift in frequency, create sidebands and collapse, and he has suggested on the basis of test particle simulation that even a weak signal whose frequency is very close to the transmitter frequency, has a significant effect on triggering of new waves, and hence the effect of weaker wave components than the main causative wavelet is not negligible and may be significant. The other possibility may be the propagation effect from the source point to the satellite receiver. Even if the association between the causative wavelet and resultant chorus element is very definite at the source region, it may be destroyed during the propagation to the spacecraft location. Of course, the hiss intensity, or to be more exact, the intensity of wavelets within the hiss band must exceed a threshold value for triggering a chorus. The contour maps of intensity with the frequency resolution of 23.25 Hz are presented in this paper in order to demonstrate the presence of wavelets, but the presence of wavelets is also checked by the vectorial A.R. method with frequency resolution of 6 Hz. Hence, we can conclude that chorus emissions can be triggered by the wavelets existing in the hiss band and that the present experimental study has given a convincing support to the terminology of hiss-triggered chorus. This work has supported experimentally very much the work by KOONS (1981) and TSUJI *et al.* (1989), and the mechanism of hiss-triggered chorus is likely to be coherent wave-particle interactions as in the case of Siple wave injection experiments. HELLIWELL *et al.* (1986) have used the Siple transmitter to simulate the magnetospheric hiss, and have presented the experimental results in which relatively short duration wavelets of a hiss spectrum is converted into the longer, semicoherent discrete emissions that are typical of chorus. The experimental findings obtained in the present paper have furthermore supported the con-

clusion by HELLIWELL *et al.* (1986). In these coherent wave instabilities, the most serious problem is the effect of other wavelets at different frequencies on the coherent wave-particle interactions. MATSUMOTO and OMURA (1981) have made the test particle simulation on phase bunching in the presence of two waves whose frequencies are slightly different from each other, but with the same amplitudes. Then, when the frequency difference $\delta\omega$ is greater than $2\omega_t$ (ω_t: trapping frequency), electrons trapped by the first wave are not detrapped by the second wave. If we take the wave amplitude as $5m\gamma$, $2\omega_t$ becomes about 30 Hz for the plasma parameters observed. The similar "control frequency" f_c is derived by DOWDEN *et al.* (1978), and this f_c is estimated by means of their expression. Then, we obtain $f_c \simeq 35$ Hz, which is in good agreement with the previous value. Hence, the wavelets near the edge of hiss band are albe to phase-bunch the resonant electrons near the equatorial plane, and these phase bunched electrons are not detrapped by another wavelet whose frequency is spaced higher than 30 Hz. But a recent study by SA (1990) has indicated that even a weak second signal whose frequency becomes very close to the transmitter signal frequency plays a significant role in triggering a new emission, and so further detailed studies in this direction will be required.

Other important outcomes from direction finding measurements (Items (4) and (5)) must be fully incorporated in the detailed mechanism of triggering chorus by hiss (HATTORI *et al.*, 1989) and further studies are in progress. Another finding on the periodicity in occurrence of chorus (Item (6)) is an interesting subject to be studied in future.

References

BENDAT, J. S. and PIERSOL, A. G. (1971): Random data; Analysis and Measurement Procedures. Wiley-Interscience.

BURTIS, W. J. and HELLIWELL, R. A. (1969): Banded chorus-A new type of VLF radiation observed in the magnetosphere by OGO 1 and OGO 3. J. Geophys. Res., **74**, 3002–3010.

BURTIS, W. J. and HELLIWELL, R. A. (1976): Magnetospheric chorus; Occurrence patterns and normalized frequency. Planet. Space Sci., **24**, 1007–1024.

BURTON, R. K. and HOLZER, R. E. (1974): The origin and propagation of chorus in the outer magnetosphere. J. Geophys. Res., **79**, 1014–1023.

CORNILLEAU-WEHRLIN, N., GENDRIN, R., LEFEUVRE, F., PARROT, M., GRARD, R., JONES, D. *et al.* (1978): VLF waves observed onboard GEOS-1. Space Sci. Rev., **22**, 371–382.

DOWDEN, R. L. (1971): Distinctions between mid-latitude VLF hiss and discrete emissions. Planet. Space Sci., **19**, 374–376.

DOWDEN, R. L., MCKAY, A. D., AMON, L. E. S., KOONS, H. C. and DAZEY, M. H. (1978): Linear and nonlinear amplification in the magnetosphere during a 6.6-kHz transmission. J. Geophys. Res., **83**, 169–181.

HATTORI, K., HAYAKAWA, M., SHIMAKURA, S., PARROT, M. and LEFEUVRE, F. (1989): Geos-1 observation of hiss-triggered chorus emissions in the outer magnetosphere and their generation model. Proc. NIPR Symp. Upper Atmos. Phys., **2**, 84–95.

HAYAKAWA, M., YAMANAKA, Y., PARROT, M. and LEFEUVRE, F. (1984): The wave normals of magnetospheric chorus emissions observed onboard GEOS-2. J. Geophys. Res., **89**, 2811–2821.

HAYAKAWA, M., OHMI, N., PARROT, M. and LEFEUVRE, F. (1986a): Direction finding of ELF hiss in a detached plasma region of the magnetosphere. J. Geophys. Res., **91**, 135–141.

HAYAKAWA, M., TANAKA, Y., SAZHIN, S. S., OKADA, T. and KURITA, K. (1986b): Characteristics of dawnside mid-latitude VLF emissions associated with substorms as deduced from the two-

stationed direction finding measurement. Planet. Space Sci., **34**, 225–243.

HAYAKAWA, M., TANAKA, Y., SHIMAKURA, S. and IIZUKA, A. (1986c): Statistical characteristics of mid-latitude VLF emissions (unstructured and structured); The local time dependence and the association with geomagnetic disturbances. Planet. Space Sci., **34**, 1361–1372.

HAYAKAWA, M., HATTORI, K., SHIMAKURA, S., PARROT, M. and LEFEUVRE, F. (1990): Direction finding of chorus emissions in the outer magnetosphere and their generation and propagation. Planet. Space Sci., **38**, 135–143.

HELLIWELL, R. A. (1965): Whistlers and Related Ionospheric Phenomena. Stanford, Stanford Univ. Press.

HELLIWELL, R. A., CARPENTER, D. L., INAN, U. S. and KATSUFRAKIS, J. P. (1986): Generation of band-limited VLF noise using the Siple transmitter; A model for magnetospheric hiss. J. Geophys. Res., **91**, 4381–4392.

KOONS, H. C. (1981): The role of hiss in magnetospheric chorus emissions. J. Geophys. Res., **86**, 6745–6754.

LAGOUTTE, D. and LEFEUVRE, F. (1985): Multispectral analysis for electromagnetic wave field component in a magnetoplasma: Application to narrow-band VLF emission. J. Geophys. Res., **90**, 4117–4127.

LEFEUVRE, F. and PARROT, M. (1979): The use of coherence function for the automatic recognition of chorus and hiss observed by GEOS. J. Atmos. Terr. Phys., **41**, 143–152.

LEFEUVRE, F., PARROT, M. and DELANNOY, C. (1981): Wave distribution function estimation of VLF electromagnetic waves. J. Geophys. Res., **86**, 2359–2375.

LEFEUVRE, F., NEUBERT, T. and PARROT, M. (1982): Wave normal distributions and wave distribution functions for ground-based transmitter signals observed on GEOS 1. J. Geophys. Res., **87**, 6203–6217.

LUETTE, J. P., PARK, C. G. and HELLIWELL, R. A. (1977): Longitudinal variations of very low frequency chorus activity in the magnetosphere: Evidence of excitation by electrical power transmission lines. Geophys. Res. Lett., **4**, 275–278.

LUETTE, J. P., PARK, C. G. and HELLIWELL, R. A. (1979): The control of the magnetosphere by power line radiation. J. Geophys. Res., **84**, 2657–2660.

MATSUMOTO, H. and OMURA, Y. (1981): Cluster and channel effect phase bunchings by whistler waves in the nonuniform geomagnetic field. J. Geophys. Res., **86**, 779–791.

MEANS, J. D. (1972): Use of the three dimensional covariance matrix in analyzing the polarization properties of plane waves. J. Geophys. Res., **77**, 5551–5559.

MUTO, H., HAYAKAWA, M., PARROT, M. and LEFEUVRE, F. (1987): Direction finding of half-gyrofrequency VLF emissions in the off-equatorial region of the magnetosphere and their generation and propagation. J. Geophys. Res., **92**, 7538–7550.

PARROT, M. and LEFEUVRE, F. (1986): Statistical study of the propagation characteristics of ELF hiss observed on GEOS-1, inside and outside plasmasphere. Ann. Geophys., **4**, 363–384.

S-300 EXPERIMENTERS (1979): Measurements of electric and magnetic wave fields and of cold plasma parameters onboard GEOS-1, Preliminary results. Planet. Space Sci., **27**, 317–339.

SA, L. A. D. (1990): A wave-particle-wave interaction mechanism as a cause of VLF triggered emissions. J. Geophys. Res., **95**, 12277–12286.

TSUJI, S., HAYAKAWA, M., SHIMAKURA, S. and HATTORI, K. (1989): On the statistical properties of magnetospheric VLF/ELF hiss. Proc. NIPR Symp. Upper Atomos. Phys., **2**, 74–83.

TSURUTANI, B. T. and SMITH, E. J. (1974): Postmidnight chorus; A substorm phenomenon. J. Geophys. Res., **79**, 118–127.

TSURUTANI, B. T., SMITH, E. J., CHURCH, J. R., THORNE, R. M. and HOLZER, R. E. (1979): Does ELF chorus show evidence of power line stimulation? Wave Instabilities in Space Plasma, ed. by P. J. PALMADESSO and K. PAPADOULOS. Reidel, Dordrecht.

WELCH, P. D. (1967): The use of fast Fourier transform for the estimation of power spectra; A method based on time averaging over short, modified periodograms. IEEE Trans. Audio Electroacoust., **15**, 70–74.

(Received July 28, 1990; Revised manuscript received November 5, 1990)